

Spatial and Temporal Variability of Light Attenuation in the Amazonian Waters

M. Costa ^a; K. Telmer ^b; E.M.L.M. Novo ^c

^aDepartment of Geography, University of Victoria, PO Box 3050, Victoria, BC, Canada - (maycira@uvic.ca)

^bSchool of Earth and Ocean Sciences, University of Victoria, Victoria, BC, Canada – ktelmer@uvic.ca

^cInstituto Nacional de Pesquisas Espaciais, São Paulo, Brazil

evlyn@ltd.inpe.br

Abstract – Quantification of hyperspectral downwelling vertical attenuation coefficient (K_d) and irradiance (E_d) in the euphotic depth (Z_{eu}) in 2005 (falling) and 2006 (rising waters) in Amazonian waters showed that K_d is higher in the blue (5-9 m^{-1}), decreasing towards the green (4-7 m^{-1}) and red (3-5 m^{-1}) part of the spectra. Further, K_{ds} are generally higher in white waters than in black and clear waters. A stepwise multiple regression analysis showed that when all the data is polled together, TSS and a_{cdom} are the main drivers of spectral K_{ds} ($R^2 \sim 0.65$; $p < 0.005$). However, when analyzing only black and clear waters Chla also explains the variability of K_{ds} ($R^2 \sim 0.96$; $p < 0.005$). The selective attenuation by the optical constituents result in maximum light reaching Z_{eu} of 1.0 to 0.5 m (white waters) is dominantly at 685nm, Z_{eu} of 1.8 to 3.0 m (black) is at 695nm, and Z_{eu} of 4.0 to 3.0 m (clear) is at 590nm.

Keywords: Amazon rivers, light attenuation, spatial-temporal variability

1. INTRODUCTION

In the Amazon, the characteristics of rainfall, type of geology and soil, type of vegetation, physical and biochemical alteration processes occurring in the catchments characterize the three main classes of waters, generally referred to as white, black, and clear waters (Sioli, 1950; Devol and Hedges, 2001). The proportion of different characteristics over the whole catchment influences the type of water (Junk and Furch, 1985). Small order streams can be mainly influenced by riparian ecosystems, whereas for high order streams, upstream and in-channel processes can dominate (McClain and Elsenbeer, 2001). In fact many of the Amazon's rivers are a mixture of these three water classes (Walker, 1990).

Conversion of forest to agriculture (Neill et al., 2001; Thomas et al., 2004) and conversion of forest and floodplains to mining operations (Roland and Esteves, 1998; Mol and Ouboter, 2003; Telmer et al., 2006), however, have resulted in an increasing in both physical and chemical erosion leading to increased amounts of particulate and dissolved compounds in Amazonian waters, and consequently the in-water light climate. Roland and Esteves (1998) and Guenther and Bozelli (2004) have shown that PAR limitation due to high concentrations of particulate compounds is the dominant factor on the reduction of the abundance of phytoplankton in the mining impacted Batata Lake, thus showing the critical importance that light plays in Amazonian aquatic ecology. This is an important start; however, because PAR is attenuated at different rates in different parts of the spectra, it is of great value to spectrally resolve how light is attenuated in the different waters. We report the spectral downwelling vertical attenuation coefficient

and irradiance from just below the water surface down to a depth in which PAR declined to 1% (Z_{eu}) in black, white, and clear water of large rivers of the Amazon Basin. This provides baseline information for most successfully understand how biological and chemical processes are affected by particular changes, either natural or human induced.

2. METHODS

2.1. Study area

Sampling was done along a 500 km E-W transect (60° 07'W to 54° 08'W) of the Amazon River, beginning upstream from the Solimões and Negro confluence to the Tapajós River, at Santarém, and from six major tributaries: Solimões, Negro, Madeira, Uatumã, Trombetas, and Tapajós. Cruises were conducted in the onset of falling and rising water periods (June 2005 and December 2006, respectively).

2.2. Water samples

Water samples were collected at 0.5 m depth at three different locations in each river, producing 27 discrete samples in 2005, and 33 in 2006. Additionally, in 2006, water samples were also collected at Z_{eu} . For both sampling campaigns, data from the three different locations were averaged to represent a river. Immediately after sampling, water was vacuum filtered onboard the boat through pre-weighed and pre-ignited GF/F 0.7 μm glass-fiber membranes to determine the concentration of total suspended solids TSS (total suspended solids) and photosynthetic pigments. TSS was determined by weight difference following the method of APHA (1998). Chlorophyll concentrations (Chla) were determined by High Performance Liquid Chromatography (HPLC) using methods adapted from EPA (1997). For determination of absorbance due to coloured dissolved organic matter, the filtrate that passed through 0.7 μm (2005 cruise) and 0.2 μm (2006 cruise) membranes was collected in pre-combusted amber glass bottles and kept cold and dark in coolers. The filtrate was analyzed spectrophotometrically for absorbance at 440nm using an Ocean Optics 2000 USD spectrophotometer with a 100mm cuvette, and the absorption coefficient of CDOM ($a_{CDOM} m^{-1}$) was calculated according to Kirk, (1994).

2.2. In situ optical data

At each of the 60 sampling locations (2005 and 2006 inclusive), vertical samples of planar irradiance were acquired with Satlantic HyperPRO spectroradiometer from subsurface to Z_{eu} . The Satlantic HyperPRO has an in-water hyperspectral radiometer (HyperOCR) to measure downwelling irradiance ($E_d(z, \lambda)$), and sensors for temperature and depth determinations.

A second hyperspectral radiometer was installed on a pole on the top of the boat to measure above-water downwelling irradiance ($E_s(\lambda)$). These radiometers operate in a calibrated spectral range from 350 to 800 nm.

Spectral data were filtered for tilt and synchronized with depth and time, and the normalized downwelling irradiance ($nE_d(z,\lambda)$) and diffuse attenuation coefficient ($K_d(z,\lambda)$) were calculated. $nE_d(z,\lambda)$ was calculated by normalizing $E_d(z,\lambda)$ to the incident irradiance $E_s(\lambda)$. Only data in which the average coefficient of variance (CV) of $E_s(\lambda)$ over time was lower than 1% were considered in the analysis. High CVs were mostly due to broken cloudy conditions. $K_d(z,\lambda)$ was defined as the linear regression coefficient of $\ln [E_d(z,\lambda) / E_s(0,\lambda)]$ with respect to depth over the depth interval just below the water surface to Z_{eu} where most of the attenuation of solar energy takes place (Kirk, 2003).

3. RESULTS AND DISCUSSION

3.1. Water constituents

At both periods of sampling the temperature profile (measured +/- 3hrs of the solar noon) from the surface to Z_{eu} showed that the euphotic layer was on average 30°C, and mostly within 0.3°C of the surface temperature; thus characterizing absence of thermal stratification within the euphotic layer. This indicates that the water constituents were nearly uniformly distributed within the mixed layer, which was clearly observed in 2006 (the 2005 data was only at sub-surface). Differences in the concentrations of optical water constituents were observed from river to river and between the two seasons of sampling (Table 1). The overall range of measured TSS was 1.6 to 66.9 mg/l and 3.2 to 217.2 mg/l for 2005 and 2006, respectively. Generally, the onset of rising waters in December 2006 was associated with an increase in at least twice of TSS compared to 2005. While this increase in concentration mostly happened in the white water rivers, the concentration in the Negro and Trombetas rivers remained similar and in the Uatuma River decreased by two folds. As such, TSS were the highest in the white waters (~ 49.0 mg/l and 155.0 mg/l, respectively for 2005 and 2006), and relatively lower for black and clear waters (Table 1). TSS values were especially high in the white waters of the Solimoes and Madeira rivers, and in the Amazon River after the confluence with these rivers. Maximum concentrations in the Solimoes and Madeira rivers happened in the early rising water stages (>170 mg/l), and minimum at falling water stages (50 mg/l). Also, at the early rising water stage we observed a tendency of decreasing TSS downstream of the Amazon River, and the opposite was observed in the falling water stage. These phenomena has been associated with the respective storage and resuspension of sediment due to changes in the surface slope of the main stem of the Amazon, which is a result of slightly different timing of peak water stages of the Amazon River and some of its tributaries, i.e., Tapajos and Madeira rivers (Meade et al, 1991; Dunne et al., 1998).

Measured a_{CDOM} values varied markedly among the different classes of rivers, but not seasonally, except for white waters. Observed ranges were from 1.6 to 10.7 m^{-1} and 1.3 to 10.3 m^{-1} for falling and rising waters, respectively. The low and high ends of the a_{CDOM} range were observed in clear and black waters, respectively. The highest a_{CDOM} was measured in the Rio Negro (> 10.0 m^{-1}). Rio Solimões and Rio Madeira,

exhibited typical lower a_{CDOM} (~ 4.5 m^{-1} and 1.6 m^{-1} , respectively for falling and rising water). a_{CDOM} decreased sharply from the values measured in the Negro River to almost half (falling water) at the Solimões River. After these two water bodies mix, the characteristic high Negro a_{CDOM} is preserved in the falling water (~ 10.6 m^{-1}) but not in the rising water stage (3.6 m^{-1}). At falling water the discharge of the Negro River was much higher than at rising waters, and consequently the a_{CDOM} contribution from this river to the Amazon River in the falling water stage was increased. Overall, a_{CDOM} shows a subtle downstream gradient. Upper stream station in the Amazon River showed higher values than downstream stations, for instance, especially in the falling water. Again, this was likely a result of mixing from the high a_{CDOM} tributaries, like Rio Negro (~ 10.7 m^{-1}), and continuous dilution by lower a_{CDOM} tributaries, like Rio Tapajós (~ 2.0 m^{-1}). Also, loss of humic and fulvic acids downstream of the Negro River input due to adsorption onto fine suspended particles from the Solimões and Madeira rivers (Ertel et al., 1986) could result in the downstream decrease of measured a_{CDOM} .

Overall, Chla values did not significantly vary with depth (CV < 20%), agreeing with the non-stratified characteristics of the narrow euphotic layer of the rivers. Also, Chla did not significantly vary (CV < 20%) among replicate stations of the same river. The Tapajos River was the exception, with variable concentrations between depths (surface and Z_{eu} in 2006) and among stations. At falling water, concentrations are higher in the clear waters of the Tapajós and Trombetas rivers (2.1 and 2.7 $\mu g/l$, respectively), and in the black waters of Negro and Uatuma rivers (1.8 and 1.2 $\mu g/l$, respectively). The concentrations significantly increased at rising waters in the Tapajós (~ 16.0 $\mu g/l$) and Uatuma (4.2 $\mu g/l$), while in the Trombetas remained approximately similar (1.5 $\mu g/l$), and in the Negro River decreased (0.6 $\mu g/l$). The high values in the Tapajos were associated with an observed phytoplankton bloom (36.4 $\mu g/l$). The white water rivers exhibits relatively lower Chla values (~ 0.4 $\mu g/l$) at both sampling periods. Slightly increase in Chla was observed in the rising water stage at the Amazon downstream station close to the Tapajós River likely due to the influence of the phytoplankton bloom encountered close to the mouth of the Tapajós River.

3.2. Light climate

The euphotic depth in June 2005 range from 0.9 to 1.8m in white and black waters compared to 2.0 to 5.6 m at clear waters. In the rising waters of 2006, Z_{eu} generally decreased to at least half of the depth measured in the falling waters of 2005. For white water Z_{eu} was ~ 0.5m, increasing towards black (1.0 to 3.4m) and clear (2.5 to 4.0) waters. The difference in euphotic depths at the two different times of the year and for the different rivers was due to how light was attenuated by the variable concentrations of the optical water constituents.

The spectral diffuse attenuation coefficients for downward irradiance (K_d) are shown in Figures 1a and 1b for 2005 and 2006, respectively. Overall, attenuation was higher in the blue part of the spectra, decreasing towards the green spectra, and increasing again into the red and near infrared spectra (>700 nm). For ease of presenting the K_d behavior, we will focus the analysis in three representative wavelengths, 490 (K_{d_B}), 550 (K_{d_G}), and 650 nm (K_{d_R}) (Table 1). We avoided shorter blue wavelengths due to observed errors associated with the in-water

measurements (signal-to-noise-ratio). K_{ds} are higher for white waters and lower for black and clear waters at the rising waters of 2006 compared to falling waters of 2005; except for the Tapajos River where K_d is higher in 2006. In 2005, $K_{d,B}$ exhibited the highest values, decreasing in about the same magnitude towards the green and red light; except in the Tapajos where $K_{d,G}$ and $K_{d,R}$ are similar. In 2006, K_d values are generally higher in any part of the spectra for white waters, and lower for black and clear waters when compared with 2005. (Table 1).

A stepwise multiple regression analysis was used to identify the optical water constituents that best explains the variability in the attenuation coefficients. Response variables included $K_{d,B}$, $K_{d,G}$, and $K_{d,R}$ and predictor variables were a_{CDOM} , TSS, and Chla. Predictor variables were only accepted in the regression equations models at $p < 0.005$. The regression models were developed considering (i) all the data combined (2005 and 2006), and (ii) separate data for each year, and for each of these conditions a division between (iii) black and clear waters and (iv) white waters. The rationale for this division was the observed trend in K_d behavior for the different water classes.

The statistical analysis suggested that when all the data representing the three different water classes was included (2005 and 2006 combined or data for each separate year) the fit of the K_d models were reasonably good ($R^2 = 0.60 - 0.77$). By contrast, the fit of the models developed for only white waters at separate years were generally not significant at a 95% confidence level. However, when all the white water data from combined years was used to develop the model, TSS showed low but still significant correlation with any spectral K_d , probably due to the increased n value. Further, the models taking into consideration all data and only 2006 data included TSS as predictor variable, indicating that when all the water classes were included this variable played an important role in defining K_{ds} . Nonetheless, when only 2005 data was included, TSS did not explain the K_d models because it co-varied with Chla (Pearson $r = -0.70$).

In summary, TSS was important in defining K_{ds} for the general water classes, however, when the models were defined only for white rivers the correlations decreased or were not significant (Pearson $r = 0.17 - 0.54$). The lack of statistical significance was possibly an artifact due to the low number of white water samples used to develop the models. With this in mind, the high diffuse attenuation coefficients in white waters were likely a result of very high TSS (~ 50.6 and 154.6 mg/l for 2005 and 2006, respectively), therefore strongly scattering light in a quasi non-selective manner and contributing to the attenuation coefficient in all PAR wavelengths. In these waters, phytoplankton was likely a minor attenuator of light. This is supported by low Chla (~ 0.4 $\mu\text{g/l}$). The relatively high a_{CDOM} (6.8 and 2.6 m^{-1}) suggested absorption of light in the blue/green wavelengths, likely playing a role on the very low level of blue light at Z_{eu} . As well, green light was present only in very low intensities, and red light was the least attenuated (lowest K_d) and therefore dominated at Z_{eu} (Figure 1 and 2).

Statistical models developed with only combined black and clear waters showed the highest R^2 ($0.80 - 0.98$). Predictor variables included in the models vary; TSS was mostly included

in the models. Situations in which either Chla or a_{CDOM} were not included in the model was due to co-variance. In the falling waters of 2005, a_{CDOM} better explained the K_d models. As such, attenuation of light was likely due to absorption by the higher content of a_{CDOM} (~ 8.6 m^{-1}) and to a less extent Chla (~ 1.4 $\mu\text{g/l}$), especially for the Negro River. CDOM, therefore, caused rapid depletion of blue light (less than 1% at Z_{eu}). On the contrary in 2006, the K_d statistical models for black and clear waters selected Chla to better explain the models. Light attenuation was therefore mostly due to absorption and scattering by high Chla, thus resulting in similar magnitude of attenuation coefficients and euphotic depth measured observed in 2005. Generally in 2006 higher values of Chla were measured compared with 2005. For both, 2005 and 2006 irradiance at Z_{eu} becomes mostly dominated by green and red light. The relatively lower $K_{d,G}$ and $K_{d,R}$ values enabled the definition of an euphotic layer twice that of white waters.

4. CONCLUSIONS

In this study, we described the in-water light field of the Amazonian rivers in their natural states, during the high (2005) and low (2006) water periods. Our results showed that in the shallow euphotic layer of white waters, photosynthetically active radiation becomes spectrally dominated by red light. This is primarily due to high attenuation by suspended particulates. In these waters, suspended particulates attenuate light in a quasi-non-selective spectral manner. Hence, blue and green radiation is non-existent below a 0.5 m depth, and red light likely maintains any photosynthetic activity at Z_{eu} . This may account for the presence of diatoms in these waters, which contain pigments that absorb a broad spectrum of light within the PAR range. Black waters showed relative similar behavior; however, dissolved organic matter was the main attenuator of light.

On the other hand, in clear waters, green and red light dominates the euphotic layer as a result of the lower attenuation coefficients at this part of the spectra due to selective attenuation by chlorophyll. Clear waters were therefore characterized by different phytoplankton communities, Cyanophyceae, which were likely taking advantage of available green light in the deeper euphotic layer of these waters.

This is a key piece of information required to understand the effect of human activities on the light field and ecology of affected waters in the Amazon Basin. With this in hand, changes in the light field as a consequence of land-use changes and resource extraction can be investigated and managed to minimize ecological damage.

REFERENCES

- APHA. 1998. Standard Methods for the Examination of Water and Wastewater, 1015 15th Street, NW, Washington, DC 20005.
- EPA. 1997. Method 447.0 Determination of chlorophyll a and b and identification of other pigments of interest in marine and freshwater algae using high performance liquid chromatography with visible wavelength detection. 20 pp.

Ertel, J.R.; Hedges, J.I.; Devol, A.H.; Richey, J.E.; Ribeiro, M.N.G. 1986. Dissolved humic substances of the Amazon River system. *Limnology and Oceanography*. 31(4):739-754.

Devol and Hedges. 2001 A.H. Devol and J.I. Hedges, Organic matter and nutrients in the mainstem Amazon River. In: M.E. McClain, R.L. Victoria and J.E. Richey, Editors, *The Biogeochemistry of the Amazon Basin*, Oxford University Press, Oxford (2001), pp. 275–306.

Dunne, T; Mertes, L.A.; Meade, R.H.; Richey, J.E.; Forsberg, B.R. 1998. Exchanges of sediment between the floodplain and channel of the Amazon River in Brazil. *GSA Bulletin*. 110(4):450-467.

Guenther, M.; Bozelli, R. 2004. Effects of inorganic turbidity on the phytoplankton of an Amazonian Lake impacted by bauxite tailings. *Hydrobiology*. 511: 151-159.

Junk, W.J.; Furch, K. 1985. The physical and chemical properties. In G.T. Prance and T. E. Lavejoy (Eds.). *Key Environments, Amazonia*. pp.3-17. Pergamon press, New York.

Kirk, J.T.O. 1994. Light and Photosynthesis in Aquatic Systems. New York: Cambridge University Press.

Kirk, J.T.O. 2003. The vertical attenuation of irradiance as a function of the optical properties of the water. *Limnology and Oceanography*. 48(1):9-17.

McClain, M.E.; Elsenbeer, H. 2001. Terrestrial inputs to Amazon streams and internal biogeochemical processing. In: M.E. McClain, R.L. Victoria and J.E. Richey, Editors, *The Biogeochemistry of the Amazon Basin*, Oxford University Press, Oxford (2001).

Meade, R.H; Royal, J.M.; Conceicao, S.C.; natividade, J.R.G. 1991. Backwater effects in the Amazon basin. *Environ. Geol. Water Sci*. 18:105-114.

Mol, J.H., P.E.Ouboter. 2003. Downstream effects of erosion from small-scale gold mining on the instream habitat and fish community of a small neotropical rainforest stream. *Conservation Biology*. 18:201-214.

Neill, C.; L.A. Deegan, S.M. Thomas, C.C. Cerri. 2001. Deforestation of pasture alters nitrogen and phosphorus in small Amazonian streams. *Ecological Applications*. 11: 1817-1828.

Roland, F., F.A Esteves. 1998. Effects of bauxite tailing on PAR attenuation in an Amazonian crystalline water lake. *Hydrobiology*. 377:1-7.

Sioli, H. 1950. Das wasser im Amazonasgebiet. *Forsch Fortschr*. 26:274-280.

Thomas, S.M., C. Neill, L.A. Deegan, A.V. Krusche, V.M. Ballester, R.L. Victoria, 2004. Influences of land use and stream size on particulate and dissolved materials in a small Amazonian stream network. *Biogeochemistry*. 68: 135-151.

Walker, I. 1990. Ecologia e biologia dos igapós e igarapés. *Ciência Hoje*. 11:44-53.

Table 1. Characteristics of the different water classes (average values).

Water class	White		Black		Clear	
	2005	2006	2005	2006	2005	2006
K_{d_B} (m^{-1})	7.1	11.9	5.3	2.4	3.2	2.5
K_{d_G} (m^{-1})	4.9	9.5	3.8	1.4	2.0	1.6
K_{d_R} (m^{-1})	3.3	8.7	2.0	0.9	1.4	1.5
Chla ($\mu g/l$)	0.4	0.4	1.4	4.2	2.4	9.9
TSS (mg/l)	49.2	154.7	8.5	4.5	2.6	3.7
a_{CDOM} (m^{-1})	6.5	2.6	8.6	1.5	3.2	1.8

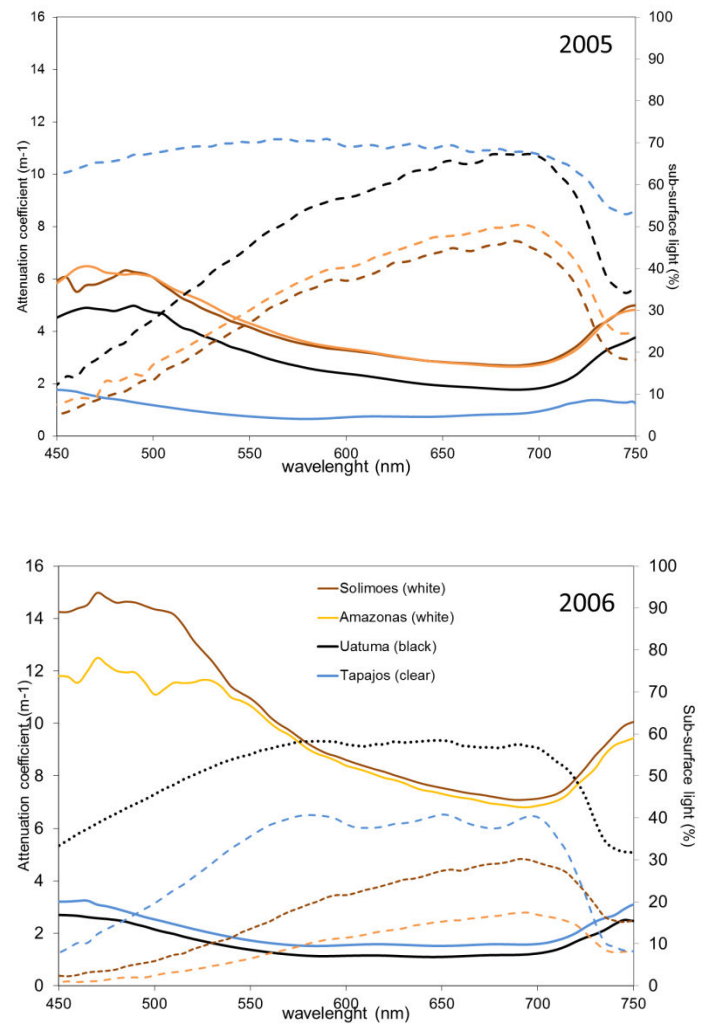


Figure 1. Attenuation coefficient and sub-surface light in representative Amazonian rivers for each class: white, black and clear. Dash and continuous lines represent sub-surface light and attenuation coefficient, respectively. (a) 2005 data and (b) 2006 data.